Diabetic Visceral Hypersensitivity Is Associated With Activation of Mitogen-Activated Kinase in Rat Dorsal Root Ganglia

Gintautas Grabauskas, Andrea Heldsinger, Xiaoyin Wu, Dabo Xu, ShiYi Zhou, and Chung Owyang

OBJECTIVE—Diabetic patients often experience visceral hypersensitivity and anorectal dysfunction. We hypothesize that the enhanced excitability of colon projecting dorsal root ganglia (DRG) neurons observed in diabetes is caused by a decrease in the amplitude of the transient A-type K^+ (I_A) currents resulting from increased phosphorylation of mitogen-activated protein kinases (MAPK) and reduced opening of $K_v4.2$ channels.

RESEARCH DESIGN AND METHODS—We performed patch-clamp recordings of colon projecting DRG neurons from control and streptozotocin-induced diabetic (STZ-D) rats. Western blot analyses and immunocytochemistry studies were used to elucidate the intracellular signaling pathways that modulate the I_A current. In vivo studies were performed to demonstrate that abnormal MAPK signaling is responsible for the enhanced visceromotor response to colorectal distention in STZ-D rats.

RESULTS—Patch-clamp studies demonstrated that I_A current was diminished in the colon projecting DRG neurons of STZ-D rats. Western blot analysis of STZ-D DRG neurons revealed increases in phosphorylated MAPK and $K_v4.2$. In diabetic DRG neurons, increased intracellular Ca^{2+} ($[Ca^{2+}]_i$), protein kinase C (PKC), and MAPK were involved in the regulation of I_A current through modulation of $K_v4.2$. Hypersensitive visceromotor responses to colorectal distention in STZ-D rats were normalized by administration of MAPK inhibitor U0126.

CONCLUSIONS—We demonstrated that reduction of the I_A current in STZ-D DRG neurons is triggered by impaired $[Ca^{2+}]_i$ ion homeostasis, and this in turn activates the PKC-MAPK pathways, resulting in decreased opening of the $K_v4.2$ channels. Hence, the PKC-MAPK–$K_v4.2$ pathways represent a potential therapeutic target for treating visceral hypersensitivity in diabetes. ***Diabetes*** **60:1743–1751, 2011**

Patients with long-standing diabetes often demonstrate visceral hypersensitivity and anorectal dysfunction. This may result in altered bowel habits, rectal urgency, and diarrhea (1–4). The pathophysiology of these conditions remains unclear. Previous studies suggest that diabetes-induced sensory neuropathies may be the consequence of increased activity of primary afferent fibers leading to an increased excitatory tone in the spinal cord (5). The spectrum of interacting ionic currents in different types of neurons appears to be important in determining the excitability of sensory neurons (6,7). The transient A-type K^+ (I_A) current is an important determinant of neuronal excitability. This current participates in the transduction of graded stimulating currents into graded firing rates (8). $K_v4.2$ channels, which are the primary molecular correlates of the I_A current in sensory neurons, are prime targets for modulation (9,10).

Sensory neuropathies in diabetes are associated with abnormal signaling in the intracellular Ca^{2+} ($[Ca^{2+}]_i$) pathway in the dorsal root ganglia (DRG) neurons. Enhanced influx of Ca^{2+} via multiple high-threshold Ca^{2+} currents and/or abnormal $[Ca^{2+}]_i$ uptake by endoplasmic reticulum occurs in sensory neurons of several models of diabetes (11–15). Increased $[Ca^{2+}]_i$ signaling has also been implicated in the pathogenesis of a variety of neurodegenerative disorders (16). We hypothesize that diabetes is associated with Ca^{2+}-mediated activation of mitogen-activated protein kinases (MAPK) that modulates the I_A current in the DRG neurons. The reduction in I_A current results in enhanced neural excitability, which may cause rectal hypersensitivity. To test this hypothesis, we examined how diabetes-evoked changes in $[Ca^{2+}]_i$ homeostasis modulate the excitability of distal colon projecting DRG neurons. We demonstrated that diabetic visceral hypersensitivity in the rectum is mediated by an abnormal I_A current resulting from increased phosphorylation of MAPK in DRG neurons. This decreases the opening of $K_v4.2$ channels and reduces the amplitude of I_A current. The increased neuronal excitability appears to be responsible for rectal hypersensitivity in diabetes.

RESEARCH DESIGN AND METHODS

All procedures were performed in accordance with the National Institutes of Health guidelines and with the approval of the University Committee on Use and Care of Animals at the University of Michigan.

Generation of streptozotocin-induced diabetic rats. Diabetes was induced in Sprague-Dawley rats (200 g) by an intraperitoneal injection of streptozotocin (STZ; 50 mg/kg) dissolved in sodium citrate buffer. Diabetes was confirmed 2–12 weeks later by measurement of tail vein blood glucose levels with Glucotide strips (Bayer Diagnostics, Puteaux, France). Only rats with a final blood glucose level >15 mmol/L (300 mg/dL) were included in the study. Control rats received only sodium citrate buffer.

Retrograde tracing of DRG neurons. Normal (n = 11) and STZ-induced diabetic (STZ-D; n = 15) male rats were deeply anesthetized with a mixture of halothane in air, as described previously (17,18). After a laparotomy, the retrograde tracer DiI was applied to the distal colon. To confine the dye to the application site, DiI crystals were embedded in a fast-hardening epoxy resin that was allowed to harden for approximately 5 min. The wound was closed with nylon sutures (4-0). The animals were allowed to recover for a 15–20-day period before being killed for the harvesting of L6–S2 DRG neurons.

Isolation and culture of DRG neurons. DRG neurons from L6–S2 spinal segments were surgically removed from rats anesthetized with ketamine (250 mg/kg) and xylazine (25 mg/kg). The ganglia were digested for 60 min at 37°C in Dulbecco's modified Eagle's media (DMEM; Invitrogen, Carlsbad, CA) containing 1 mg/mL dispase (Roche, Nutley, NJ) and 1 mg/mL collagenase type I (Invitrogen). Neurons were dispersed by gentle trituration through Pasteur pipettes and washed with DMEM. Droplets of media containing isolated DRG

From the Gastroenterology Research Unit, Department of Internal Medicine, University of Michigan, Ann Arbor, Michigan.
Corresponding author: Chung Owyang, cowyang@med.umich.edu.
Received 27 October 2010 and accepted 8 March 2011.
DOI: 10.2337/db10-1507

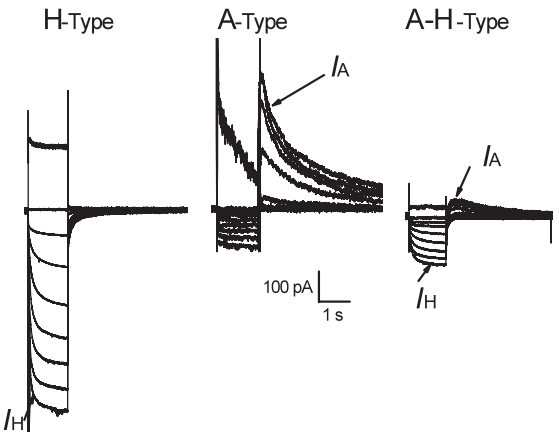

FIG. 1. Representative voltage-clamp recordings show three types of DRG neurons with the expressed I_H, I_A, or both I_H and I_A currents.

TABLE 1
Statistical analyses of the three different DRG neuronal types

	H-type	A-type	A–H-type
R_{in} (MΩ)	162 ± 28#	255 ± 55*	373 ± 70*
V_m (mV)	61.2 ± 0.7	62.1 ± 1.8	61.6 ± 1.5
AP			
Amplitude (mV)	92 ± 4.5	90.1 ± 3.7	98 ± 8.4
Duration at 50% (ms)	1.3 ± 0.3#	2.2 ± 0.4*	3.6 ± 1.0*
Threshold (pA)	240 ± 59#	54 ± 19*	233 ± 86*#
Amplitude (pA)			
I_H	353 ± 61#	Not detected*	62 ± 17*#
I_A	Not detected#	411 ± 57*	54 ± 14*#
Size (μm)	40.7 ± 7.3	29 ± 3.2	20 ± 1.5*#
% (n)	40 (32/80)	45 (36/80)	15 (12/80)

Results are expressed as mean ± SE. The significance of differences was determined with the Student t test, assuming unequal variance ($P < 0.05$), from three different experiments. *Significantly different from H-type. #Significantly different from A-type.

neurons were transferred onto coverslips coated with poly-D-lysine for 30 min. To mimic the ambient glucose concentrations in control and diabetic rats, isolated DRG neurons from control and STZ-D rats were maintained in 5 or 15 mmol/L glucose containing DMEM/F12 media, respectively, supplemented with 10% fetal calf serum (Invitrogen) and gentamycin (100 units/mL; Invitrogen) at 37°C in a 5% CO_2 atmosphere. Electrophysiological recordings on primary neuron cultures were performed within 24 h.

Patch-clamp electrophysiology. Labeled DRG neurons were identified using a Nikon Ti-S microscope equipped with TRITC epifluorescence filters. Whole-cell or perforated patch recordings were performed using borosilicate glass electrodes with resistance between 3 and 6 mol/LΩ (A-M Systems, Sequim, WA) backfilled with a saline solution composed of 130 mmol/L potassium gluconate, 10 mmol/L HEPES, 10 mmol/L EGTA, 1.0 mmol/L $MgCl_2$, 2.5 mmol/L $CaCl_2$, 1.0 mmol/L adenosine triphosphate, and 0.3 mmol/L guanosine triphosphate. Current and voltage recordings were obtained from discrete isolated DRG neurons using the Axopatch 200B patch-clamp amplifier (Axon Instruments, Foster City, CA). The signals were digitized using the analog-to-digital converter Digidata 1322B (Axon Instruments) and then stored and analyzed on a personal computer running pClamp 10 software. The membrane resistance of DRG neurons was calculated in current clamp mode by measuring membrane potential changes in response to the current step of 20-pA amplitude and lasting 500 ms. The resting membrane potential (V_M) of each cell was recorded from the voltage meter in current clamp mode at the beginning of each experiment. An action potential (AP) was evoked by injecting depolarizing current pulses while keeping the DRG neurons at approximately −60 mV by a constant current injection. The amplitude of command current was increased in 10-pA increments until it reached sufficient intensity to initiate an AP. AP duration was measured at half-peak amplitude. The amplitudes of I_A and I_H, a slowly activating current evoked by hyperpolarization, were measured in voltage clamp mode. I_H was evoked by a hyperpolarizing voltage command to −130 mV from a holding potential of −60 mV. I_A was evoked on repolarization to a holding potential (−60 mV) from the test hyperpolarization to −130 mV. The amplitude was measured at its peak current.

Measurement of $[Ca^{2+}]_i$. DiI-labeled neurons were identified by the intracellular presence of red label using TRITC filter. These DRG neurons plated on glass coverslips were incubated in physiological saline containing 2 μmol/L Fura-2-acetoxymethyl ester (Molecular Probes, Eugene, OR) for 15 min at 37°C. The dish volume was subsequently reduced to 0.5 mL, and the cells were equilibrated in physiological saline at a flow rate of 1 mL/min in a heated chamber (30–33°C). After >10 min, the fluorescence of individual DRG neurons was elicited by alternating excitation wavelengths of 340 and 380 nm (Till Polychrome V; Till Photonics, Gräfelfing, Germany) using a 410-dichroic longpass beamsplitter and a D510/80-wide band emission filter. Neuron images were captured at 510 nm using a Nikon camera. The camera and monochromator were controlled by NIS-Elements imaging software, and the concentrations of $[Ca^{2+}]_i$ were calculated online. The software allows subtraction of background fluorescence. The actual $[Ca^{2+}]_i$ was calculated from the ratio of fluorescence recorded at excitation wavelengths of 340 and 380 nm.

Western blot analyses. DRG neurons from L6–S2 were lysed and centrifuged at 14,000*g* for 10 min. Protein samples were then run on Ready Gel 12% Tris-HCl for 1.5 h at 80 V. Proteins were then transferred to nitrocellulose membranes for 1 h at 80 V. The membranes were blocked with StartBlock buffer T20 for 1 h at room temperature, probed with primary antibodies that recognize either anti-MAPK or anti-phospho–p44/p42 MAPK (extracellular signal-regulated kinase [Erk]1/2) after activation by dual phosphorylation at Thr202/Tyr204 (Cell Signaling Technology, Danvers, MA). The later studies were performed at 1:1,000 dilution at 4°C overnight and then washed in Tris-buffered saline with 0.1% Tween 20 for 1 h. To measure the levels of $K_v4.2$ channels, we used anti-$K_v4.2$ or anti-phospho–$K_v4.2$, which detects phosphorylation on Thr602 (Santa Cruz Biotechnology, Inc., Santa Cruz, CA) at 1:1,000 dilution at 4°C overnight and then washed in Tris-buffered saline with 0.1% Tween 20 for 1 h. The membranes were probed with corresponding horseradish peroxidase–conjugated secondary anti-rabbit antibodies at 1:2,000 dilution. Protein bands were detected with enhanced chemiluminescence Western blotting reagents (Thermo Fisher Scientific, Rockford, IL). The resulting bands were scanned with an Epson 2400 printer and analyzed using the ImageJ program.

Immunohistocytochemistry studies. Immunohistocytochemistry studies to localize MAPK/Erk(1/2), $K_v4.2$, and neurofilament marker (NF200) were performed in L6–S2 DRG neurons from control rats (n = 3) and STZ-D rats (6–8 weeks after induction of diabetes; n = 3). After anesthesia with urethane, a transcardial perfusion was performed with ice-cold, heparinized PBS and subsequently with a fixative containing 4% paraformaldehyde, 0.2% picric acid, and 0.35% glutaraldehyde in phosphate buffer (0.1 mol/L, pH 7.4). The DRG neurons were removed and placed in the same fixative for 2 h at room temperature and then in 25% sucrose in PBS (0.1 mol/L) overnight at 4°C. Sections (5–10 μmol/L) of the DRG neurons were incubated in 5% normal donkey serum in PBS for 1 h at room temperature. Labeling was performed using mouse monoclonal anti-$K_v4.2$ (K57/1; University of California at Davis, National Institutes of Health NeuroMab facility, Davis, CA) dilution 1:500 and rabbit anti-phospho–p44/42 MAPK(Erk1/2) (Thr202/Tyr204; Cell Signaling Technology) dilution 1:500. The primary antibodies were diluted in PBS containing 2% normal donkey serum and 0.3% Triton X-100, and tissues were incubated overnight at room temperature. The tissues were washed in PBS and exposed for 1 h to species-specific AlexaFluor 488 (Molecular Probes) or cyanine 3-conjugated secondary antibodies (Jackson ImmunoResearch Laboratories, West Grove, PA) diluted with PBS containing 0.3% Triton X-100. Specificity of immunohistochemical labeling was verified with the omission of primary antibodies, and staining was performed using only secondary antibodies. The sections were coverslipped and then sealed.

Visceromotor responses to graded colorectal distention. Measurement of visceral sensitivity in animals was mainly based on brain stem reflexes, which have been described as pseudoaffective responses (19). The visceromotor responses were recorded by quantifying a reflex contraction of the abdominal musculature induced by colorectal distention (CRD). The animals were anesthetized with a mixture of xylazine and ketamine (13 and 87 mg/kg body wt, respectively). Electromyography electrodes were implanted into the external oblique pelvic muscles 4–6 days before the beginning of the experimental procedures. The skin was sutured over the strain gauge, and the lead wires were looped around the animal's flank and secured with a single suture in the skin. During the experiment, the strain gauge was connected by way of a shielded cable to a chart recorder to monitor the number of abdominal muscle contractions. A latex balloon (7 cm long) was be inserted into the colon through the rectum. Graded-pressure CRD was produced by rapidly injecting warm saline (37°C) into the colonic balloon over 1 s and maintaining the distention for 20 s. Pressure was regulated with a distention control device and monitored by use of a pressure transducer. Graded-intensity stimulation trials (20–40–60–80 mmHg CRD) were conducted to establish stimulus-response

curves. Each distention trial consisted of three segments: a 20-s predistention baseline period, a 20-s distention period, and a 20-s post-CRD termination period with a 4-min interstimulus interval. The responses were considered stable if there was less than 20% variability between two consecutive trials of CRD at 60 mmHg. The results of electromyography were amplified and filtered (5,000×, 300–5,000 Hz; A-M Systems), digitized, and integrated by using the SPIKE2/CED 1401 data-acquisition interface. Spike bursts higher than 0.3 mV were regarded as significant and were, therefore, used to estimate the pain response.

Visceromotor responses were performed in both control and U0126-treated rats. U0126 was administered either intravenously (10 μg/kg) or intrathecally (5 μg in 0.5 μl of saline). For intrathecal administration, rats were anesthetized, and a 25-gauge, 1-inch needle connected to a 20-μl Hamilton syringe was inserted into the subarachnoid space between lumbar vertebrate S1 and S2 until a tail-flick was elicited. The syringe was held in the position for a few seconds after injection.

Statistical analysis. Data were presented as mean ± SEM; n is the number of samples. The software package InStat 3 (GraphPad Software, Inc., San Diego, CA) was used for data analysis. The χ^2 tests were used for analyses of contingency tables with more than three categories. For analysis of differences between means, one-way ANOVA with Student-Newman-Keuls test was used. Results were considered statistically significant when $P < 0.05$.

RESULTS

Basic electrophysiological properties of DRG neurons. Whole-cell recordings were obtained from 80 DRG neurons, 45 of which were labeled after placement of DiI in the distal colon. DRG neurons were divided into three groups on the basis of expression of fast inactivation of I_A and I_H currents. The H-type neurons, comprising 45% of the total population of isolated DRG neurons, were characterized as a group of neurons that expressed I_H and no I_A current. In comparison, the A-type neurons (40%) expressed I_A and no I_H current, and the A–H-type group (15%) expressed both I_H and I_A currents (Fig. 1). The general electrophysiological properties of these three groups of neurons are provided in Table 1.

No significant differences in neuronal properties were observed between DiI-labeled and nonlabeled neurons (data not shown).

Effect of diabetes on I_A current in DRG neurons. Among the three groups of distal colon projecting neurons, only A-type neurons appeared to be affected by diabetes as demonstrated in STZ-D rats (6–8 weeks after induction of diabetes) (Fig. 2*A*). The density of I_A current was significantly smaller in STZ-D A-type neurons when compared with controls (Fig. 2*B*). STZ-D did not alter the I_A current-voltage relationship (Fig. 2*C*).

Increase in phosphorylation of MAPK(Erk1/2) and K_v4.2 in diabetic DRG neurons. The K_v4.2 channel that mediates the I_A current is specifically phosphorylated at Thr602 by MAPK(Erk1/2), resulting in decreased opening of the channel and neuronal depolarization (20,21). We investigated whether the phosphorylation of MAPK isoforms Erk1/2 and K_v4.2 were enhanced with the development of diabetes. Immunoblot analysis with specific anti-phospho–44/42 MAPK(Erk1/2) and anti-phospho–K_v4.2 revealed a progressive increase in the levels of phosphorylation of MAPK(Erk1/2) and K_v4.2 in diabetic DRG neurons. At 8 weeks, the phosphorylated-MAPK (*p*-MAPK) and phosphorylated-K_v4.2 (*p*-K_v4.2) levels were 240 ± 19 and 265 ± 31% above the levels in nondiabetic age-matched DRG neurons ($P < 0.05$; Fig. 3). In contrast, the levels of nonphosphorylated K_v4.2 did not change with diabetes

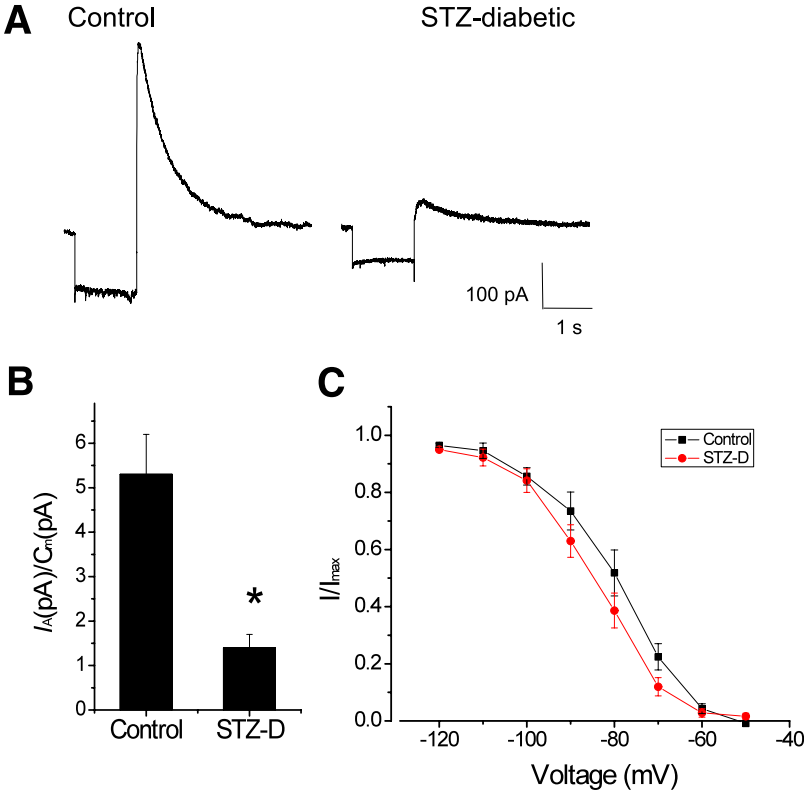

FIG. 2. Effects of STZ-induced diabetes on the amplitude of I_A current in A-type DRG neurons. *A:* Representative recordings of I_A currents in control and STZ-D DRG neurons. *B*: Summary histogram shows that the amplitude of I_A current normalized to cell capacitance (C_m) was significantly reduced in STZ-D (6–8 weeks after the induction of diabetes; n = 28) neurons compared with controls (n = 24). *$P < 0.05$ compared with aged-matched controls. *C*: Normalized I_A amplitude-voltage relationships demonstrate that STZ-D (n = 11) did not affect inactivation curve compared with control (n = 11).

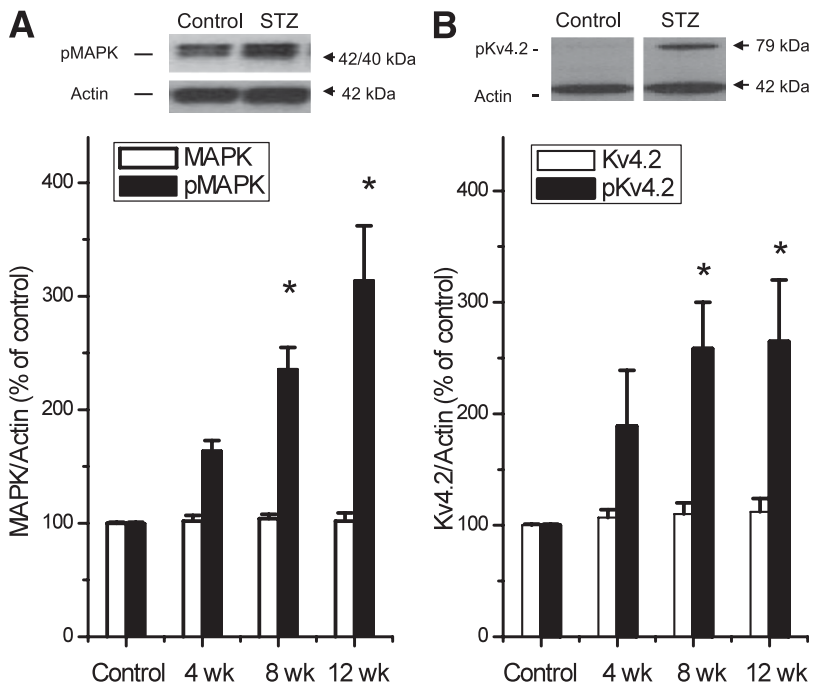

FIG. 3. Western blot demonstration of increased levels of phosphorylated-MAPK (*p*-MAPK; Erk1/2) and phosphorylated-K_v4.2 (*p*-K_v4.2) in DRG neurons of STZ-D rats. *A*: Immunoblots show increased phosphorylation of Erk1 and Erk2 in DRG homogenates from STZ-D rats 8 weeks after the induction of diabetes compared with age-matched control rats. The immunoreactive bands for MAPK and *p*-MAPK were normalized against a loading control (actin; *upper panel*). Summary histogram shows diabetes duration–dependent phosphorylation of MAPK(Erk1/2) in DRG neurons (*lower panel*; $n = 5$ for each group). *B*: Immunoblots show increased phosphorylation of K_v4.2 channel in DRG homogenates from the same group of diabetic rats compared with age-matched controls. Histogram shows diabetes duration–dependent phosphorylation of K_v4.2 in DRG neurons (*lower panel*; $n = 5$ for each group). *$P < 0.05$ compared with aged-matched controls.

(Fig. 7*C*). Immunocytochemistry showed that a large population of DRG neurons from control rats expressed the K_v4.2 channel (Fig. 4*A*-*C*). However, only a small fraction (3 ± 1%) of DRG neurons from the control group was immunoreactive to anti-*p*-MAPK(Erk1/2). This finding is consistent with that reported by Averill et al. (22). In STZ-D rats (8 weeks after induction of diabetes), the number of *p*-MAPK immunoreactive neurons was ~12 times higher (36 ± 5%) compared with that in control rats (Fig. 4*D*; $P < 0.05$). These findings indicate that phosphorylation of MAPK(Erk1/2) and K_v4.2 occurs in diabetic DRG neurons, raising the possibility that this pathway may be involved in the pathogenesis of diabetic sensory neuropathy.

$[Ca^{2+}]_i$ modulates the amplitude of the I_A current. Studies from animal models of diabetes and from diabetic patients reveal that $[Ca^{2+}]_i$ is increased in most tissues, including DRG neurons (11,20). To confirm and expand these observations, we measured the levels of resting $[Ca^{2+}]_i$ in retrograde-labeled DRG neurons isolated from control and STZ-D rats. The level of $[Ca^{2+}]_i$ was significantly increased in DRG neurons from STZ-D rats, 8 weeks after the induction of diabetes (Fig. 5*A*). We next investigated the effects of $[Ca^{2+}]_i$ on the amplitude of I_A current. Application of ionomycin (1 μmol/L), a Ca^{2+} ionophore, inhibited the amplitude of I_A by ~50% in normal retrograde-labeled DRG neurons (Fig. 5*B* and *C*). In contrast, superfusion of retrograde-labeled DRG neurons with Ca^{2+}-free solution resulted in an increase of the I_A amplitude (Fig. 5*D*). These findings indicated that $[Ca^{2+}]_i$ modulates the amplitude of I_A. We next examined the hypothesis that increased $[Ca^{2+}]_i$ acts via PKC to cause a reduction in the amplitude of I_A current. Retrograde-labeled A-type DRG neurons from normal rats were dialyzed with a specific PKC inhibitor, calphostin C (5 μmol/L), for 10–15 min ($n = 4$). At the concentration of 5 μmol/L, calphostin C acts as a specific inhibitor of PKC, which interacts with the protein's regulatory domain by competing at the binding site of diaglycerol and phorbol ester. Calphostin C effectively blocked the inhibitory effect of ionomycin, suggesting that $[Ca^{2+}]_i$ inhibits I_A current via a PKC-activated pathway (Fig. 5*E*).

Intracellular pathways responsible for modulation of I_A current. Patch-clamp whole-cell recordings of isolated distal colon projecting neurons showed that extracellular application of phospholipase C (PLC) activator (1 μmol/L; $n = 6$) inhibited the amplitude of I_A by 82% ($P < 0.05$). PLC activator is a novel sulfonamide compound that acts as a cell permeable–specific activator of PLC. The effect of the PLC activator was markedly attenuated by inclusion of calphostin C (1 μmol/L; $n = 6$), a selective PKC inhibitor, into the recording electrode (Fig. 5*F*). Furthermore, we demonstrated that PKC activation by phorbol 12-myristate 13-acetate (PMA; 1 μmol/L; $n = 5$), a phorbol ester, inhibited the amplitude of I_A by 97% ($P < 0.05$). The effect of PMA was blocked by simultaneous application of the MAPK kinase inhibitor PD98059 (1 μmol/L; $n = 4$; Fig. 5*F*) or U0126 (5 μmol/L; $n = 3$; data not shown). These data led us to conclude that the activation of the PKC-MAPK pathway by increased $[Ca^{2+}]_i$ leads to subsequent inhibition of the amplitude of I_A current.

MAPK kinase inhibitor restores the amplitude of I_A in diabetic DRG neurons. If the activation of MAPK is a necessary step for the phosphorylation of the K_v4.2 channel leading to inhibition of I_A current (22,23), inhibition of this protein kinase cascade should attenuate the

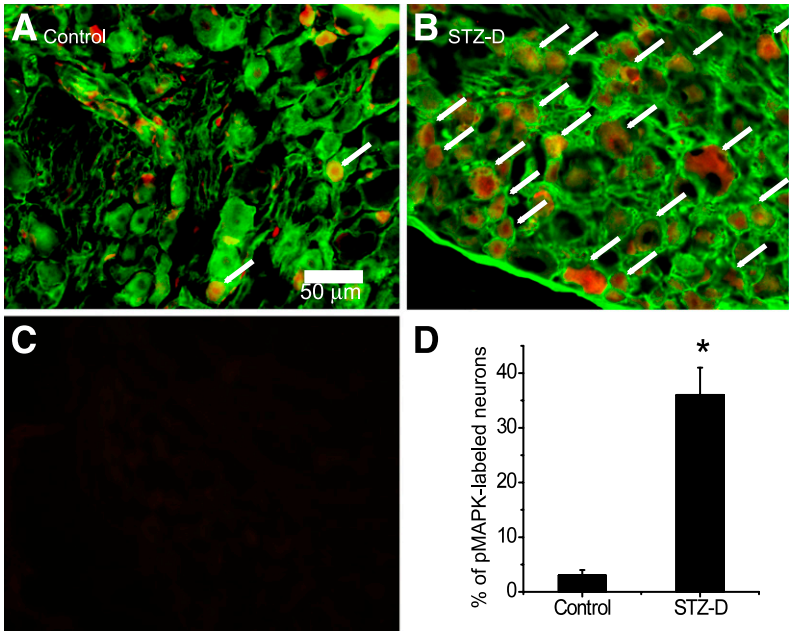

FIG. 4. STZ-induced diabetes increases the number of *p*-MAPK(Erk1/2) immunoreactive DRG neurons. Photomicrographs of merged images show colocalization of anti-K_v4.2 (green) and anti-*p*-MAPK (red) immunoreactivities from control (*A*) and STZ-D (*B*) rats DRG neurons, respectively. Note that a large population of DRG neurons from control rats expressed the K_v4.2 immunoreactivities, but only a small fraction of DRG neurons was immunoreactive to anti-*p*-MAPK (Erk1/2; arrows). Note that the number of *p*-MAPK immunoreactive neurons was ~12 times higher in STZ-D DRG compared with control DRG. *C*: Photomicrograph showing background immunoreactivities of secondary antibodies anti-mouse (green) and anti-rabbit (red) when first antibodies were omitted. *D*: Summary histogram showing the fractions of *p*-MAPK-positive neurons in control and STZ-D DRG. *$P < 0.01$, compared with control; $n = 3$. (A high-quality digital representation of this figure is available in the online issue.)

effects of STZ-induced diabetes on the amplitude of I_A. To show that MAPK is involved in diabetes-induced reduction of I_A amplitude, we examined the effects of MAPK kinase (MEK) inhibitor U0126 on DiI-labeled DGR neurons obtained from STZ-D rats 8 weeks after the induction of diabetes. Extracellular superfusion of U0126 (5 μmol/L; $n = 5$) significantly increased the amplitude of I_A (260 ± 23%; $P < 0.05$; Fig. 6*A* and *B*). To demonstrate the role of a K_v4.2 subunit in the mediation of I_A current, we measured the levels of both *p*-MAPK and *p*-K_v4.2 before and after application of U0126. Western blot analyses showed that 15-min treatment of STZ-D DRG primary neuronal cultures with U0126 (5 μmol/L; $n = 4$) significantly decreased the levels of both *p*-MAPK and *p*-K_v4.2 compared with untreated cultures (Fig. 6*C*). Similar results were obtained with another MAPK kinase inhibitor, PD98059 (data not shown).

In vivo administration of a MAPK inhibitor normalizes colorectal hypersensitivity in diabetic rats. To provide direct evidence that MAPKs contribute to the development of visceral hypersensitivity in the distal colon of diabetic rats, visceromotor responses to CRD were studied in normal ($n = 6$), STZ-D (8 weeks after STZ injection; $n = 6$), and U0126-treated STZ-D rats ($n = 6$). A significant increase in visceromotor responses occurred in STZ-D rats compared with control rats after CRD of 20, 40, and 60 mmHg. We used U0126 to inhibit MAPK activity in the DRG neurons, but not in the central neurons. U0126 does not cross the blood-brain barrier, but it can access DRG neuron somas and afferent fibers (24). Intravenous injection of U0126 (10 μg/kg; $n = 6$) in STZ-D rats significantly suppressed visceromotor responses to CRD within 15 min (Fig. 7*A*; $P < 0.05$). Similar results were obtained with intrathecal administration of U0126 (5 μg in 0.5 μl saline; Fig. 7*B*; $P < 0.05$). In contrast, intravenous injection of U0124, an inactive form of U0126, did not have any significant effect on the enhanced visceromotor responses to CRD in STZ-D rats ($n = 3$; data not shown). We also showed that intravenous administration of U0126 markedly reduced phosphorylation of Erk1/2 and K_v4.2 in L6–S2 DRG neurons (Fig. 7). These data indicate that activation of the MEK-MAPK/ERK pathway in DRG neurons plays an important role in the mediation of visceral hypersensitivity induced by diabetes.

DISCUSSION

It is well established that the diabetic state can increase the excitability of nociceptive afferents, resulting in painful diabetic neuropathy and mechanical allodynia in diabetic patients, as well as in diabetic animal models (3). On the other hand, it also has been reported that diabetes impairs the detection of lower intensity coetaneous stimuli. This effect is mediated by pelvic afferent nerve endings, which underlie low-threshold mechanosensitivity (1). The different effects of diabetes in different groups of DRG neurons and the variable duration of diabetes used in different studies may contribute to these seemingly opposite findings. The descending colon and rectum in the rat are innervated by visceral afferents that project in the pelvic (parasympathetic) nerve to the L6–S2 spinal segments (17,25). In this study, we showed that visceromotor responses to CRD were significantly higher in STZ-D rats 8 weeks after the induction of diabetes. This observation was consistent with our in vitro observations using isolated distal colon projecting DRG neurons, suggesting the development of visceral hypersensitivity.

Our electrophysiological data indicate the presence of distinct populations of DRG neurons that probably serve different physiological functions. Variation in I_H, I_{IR} (inward

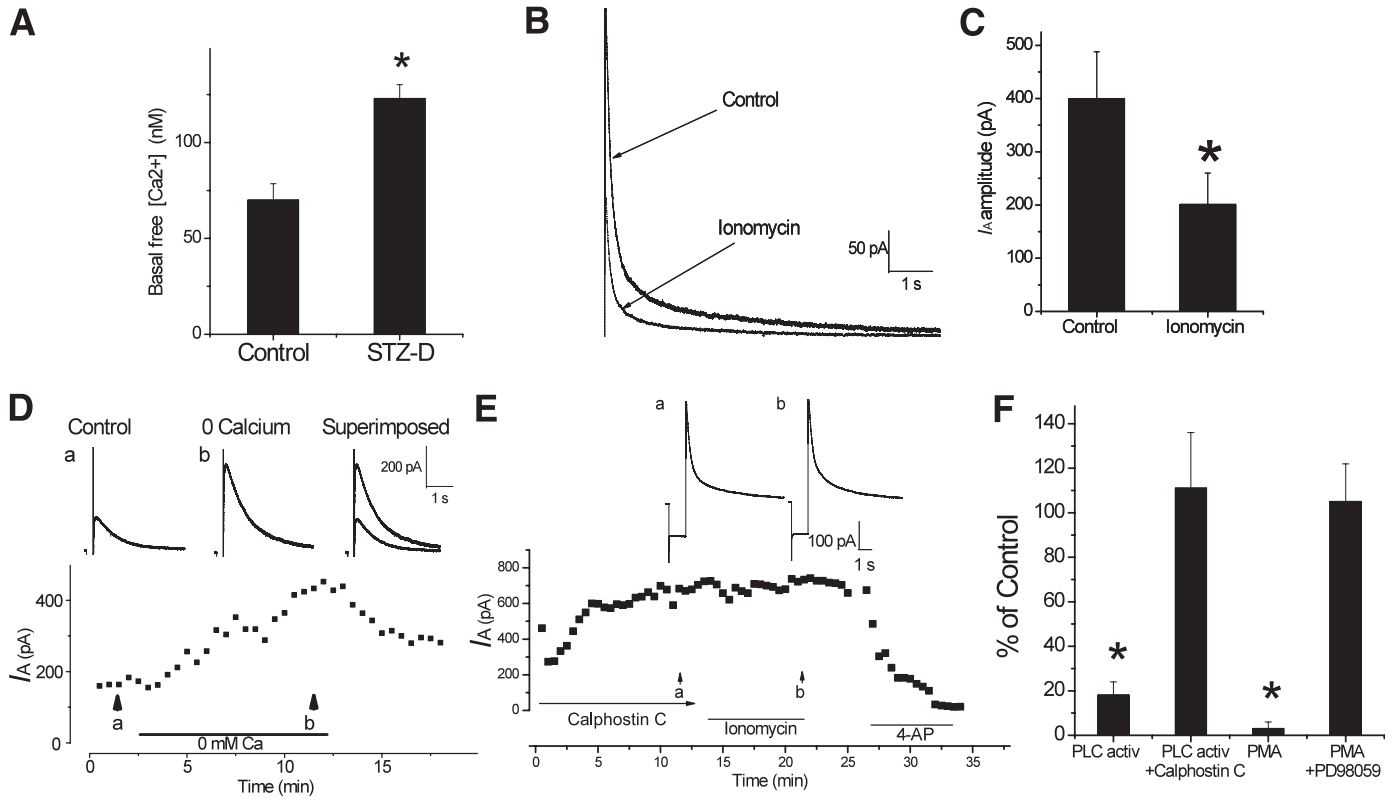

FIG. 5. $[Ca^{2+}]_i$ modulates the amplitude of I_A current in DRG neurons. *A*: Basal $[Ca^{2+}]_i$ in retrograde-labeled DRG neurons from control (n = 26) and STZ-D (n = 25) animals. *P < 0.05 from control. *B*: Superimposed current traces of I_A recorded from normal DRG neurons in control conditions and during extracellular superfusion of ionomycin (1 μmol/L). *C*: Summary histogram shows the effect of ionomycin on the amplitude of I_A current. *P < 0.05 from control. *D*: Time course of the amplitudes of I_A current plotted against time shows that bath application of Ca^{2+}-free extracellular media resulted in a progressive increase in the amplitude of I_A current. The insets show I_A current recorded in control (*upper left*) and 10 min after superfusion of Ca^{2+}-free bath media (*upper middle*). *E*: Time course of the amplitudes of I_A current plotted against time shows that dialysis of the recorded neuron with PKC inhibitor calphostin C resulted in an increase in amplitude of I_A, which became stable in 10 min (a; *upper left* inset). In the presence of calphostin C, extracellular superfusion of inomycin (1 μmol/L) did not induce a change in the amplitude of I_A current (b; *upper right* inset) and application of 4-AP (4-aminopyridine) completely abolished the amplitude of I_A current. Inhibition of I_A current by PKC is MAPK (Erk1/2)-dependent. *F*: Summary histogram shows the effects of PLC activator (1 μmol/L) and PKC activator PMA (1 μmol/L) on I_A current in control and in the presence of PKC inhibitor (calphostin C; 1 μmol/L) and MAPK kinase inhibitor (PD98059; 1 μmol/L), respectively. *P < 0.05 from control.

rectifying), and I_{leak} currents has been observed in DRG neurons of different sizes (6,7). Our data also indicated that small- and medium-sized DRG neurons preferentially express I_A current. These small- and medium-sized DRG neurons are the primary sensory neurons responsible for pain sensation (9,26). Our STZ-D rat model showed that A-type DRG neurons were affected by diabetes, resulting in the reduction of the amplitude of I_A current and enhanced excitability.

Peripheral axons and somas of sensory DRG neurons exist outside the protection of the blood–nerve barrier; thus, they are directly exposed to the high glucose levels in diabetes (5). Schneider et al. (27) reported that hyperglycemia increased the depolarizing after-potentials that caused hyperexcitability of sensory DRG neurons. Our studies further identified that I_A currents were reduced in diabetic DRG neurons.

Several studies have shown that the level of cytosolic Ca^{2+} increases with the onset of diabetes (12–15). It has been suggested that elevation of the $[Ca^{2+}]_i$ level observed in spinal sensory neurons in rodent models of diabetes is the result of increased Ca^{2+} release from internal stores and impaired Ca^{2+} resequestration (14,15). Diabetes is also associated with increased amplitude in multiple voltage–dependent Ca^{2+} currents (13–15). Disturbances in the homeostasis of $[Ca^{2+}]_i$ have been proposed to be a common pathway in the pathogenesis of neurologic complications of diabetes (12). Our studies showed that the level of $[Ca^{2+}]_i$ was significantly increased in diabetic DRG neurons, and this was associated with a reduction of I_A current.

We propose that reduction of I_A current in DRG neurons of STZ-D rat is triggered by impaired $[Ca^{2+}]_i$ homeostasis and activation of the PKC-MAPK pathway reducing the opening of $K_v4.2$ channels. This hypothesis was supported by experiments showing that administration of a MAPK kinase inhibitor normalized the levels of p-MAPK and p-$K_v4.2$ and restored the amplitude of I_A.

The expression of MAPKs is altered by high glucose and oxidative stress in cultured sensory neurons from diabetic rats (28–30). Activation of MAPK plays a key role in the regulation of central sensitization resulting in long-term pain hypersensitivity (30,31,32). Daulhac et al. (33) reported that the development of mechanical hyperalgesia, a symptom of diabetic neuropathy, in STZ-D rats correlated with an increase in MAPK phosphorylation in the spinal cord and DRG neurons. However, it is unknown whether this abnormal intracellular signaling occurs in visceral hypersensitive state in diabetic rat models. We confirmed and expanded these observations to DRG neurons

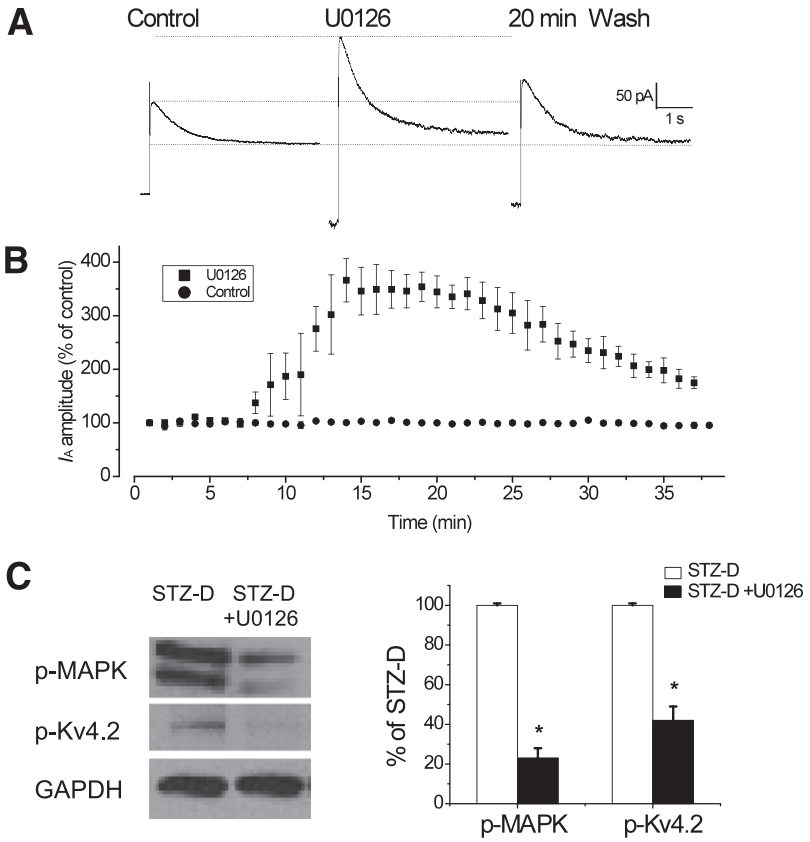

FIG. 6. Demonstration that MAPK modulates the amplitude of I_A current in STZ-D DiI-labeled DRG neurons *A*: MAPK kinase inhibitor U0126 increased the amplitude of I_A current in DRG neurons from STZ-D rats, 8 weeks after the induction of diabetes. Sample current traces were obtained before (i.e., control), at the end of application of U0126 (5 μmol/L), and after a 20-min washout. *B*: Time course of the normalized amplitudes of I_A current (mean ± SE) plotted against time shows that U0126 (5 μmol/L) normalized I_A current in diabetic DRG neurons (n = 5). *C*: Western blot shows that MAPK kinase inhibitor U0126 (5 μmol/L) inhibited both p-MAPK and p-K_v4.2 in cultured STZ-D neurons (left). Summary histogram shows the effect of U0126 on the levels of p-MAPK and p-K_v4.2 (n = 4; right). *$P < 0.05$ compared with untreated DRG neurons from STZ-D rats.

innervating the distal colon and showed that increased levels of both p-MAPK/Erk1/2 and p-K_v4.2 were detected as early as the 8th week and increased with the progression of diabetes. Furthermore, we showed that stimulation of the MAPK-PKC pathway reduced the opening of K_v4.2 channels, resulting in a reduction of the amplitude of I_A current and increased excitability. This finding should be contrasted with a recent study by Cao et al. (34) who reported that a decrease in I_A current was accompanied by a decreased gene expression in K_v4.2 in painful diabetic neuropathy. Our studies showed similar reduction of I_A current but an increase in phosphorylated K_v4.2 and no change in total protein expression. It is not uncommon that the levels of mRNA do not always correlate with the protein levels.

We provide direct evidence that MAPK contribute to the development of visceral hypersensitivity in diabetic rats. Eight weeks after the induction of diabetes, significant increase in visceromotor responses occurred in STZ-D rats after CRD of 20, 40, and 60 mmHg. This indicates the development of allodynia and hyperalgesia with a time course consistent with the increased expression of phosphorylated MAPK and K_v4.2. Most importantly, the enhanced visceromotor responses to colorectal distension in STZ-D rats were normalized by intravenous as well as intrathecal administration of the MAPK inhibitor U0126. It is interesting to note that systemic administration of U0126 in diabetic rats reduced visceromotor responses to values below those observed in normal rats. This suggests that the PKC-MAPK pathways in the DRG may play an important role to regulate rectal sensitivity even under normal physiological conditions.

In conclusion, we provide evidence for the first time that diabetic visceral hypersensitivity is mediated by abnormal I_A current resulting from increased phosphorylation of MAPK and K_v4.2 in DRG neurons. Our in vitro studies also provide evidence that increased $[Ca^{2+}]_i$ contributes to DRG neuronal excitability by activation of the PKC-MAPK pathway, resulting in decreased opening of K_v4.2 channels. These data suggest that the PKC-MAPK pathway represents a potential therapeutic target for the treatment of visceral hypersensitivity in diabetes.

ACKNOWLEDGMENTS

These studies were supported by the National Institutes of Health grants P30-DK-34933, R01-DK-084039, and R01-DK-58913 (to C.O.).

No potential conflicts of interest relevant to this article were reported.

G.G. helped with study concept and design, acquisition of data, analysis and interpretation of data, drafting of the manuscript, and statistical analysis. A.H., X.W., D.X., and S.Z. helped with acquisition of data. C.O. helped with study

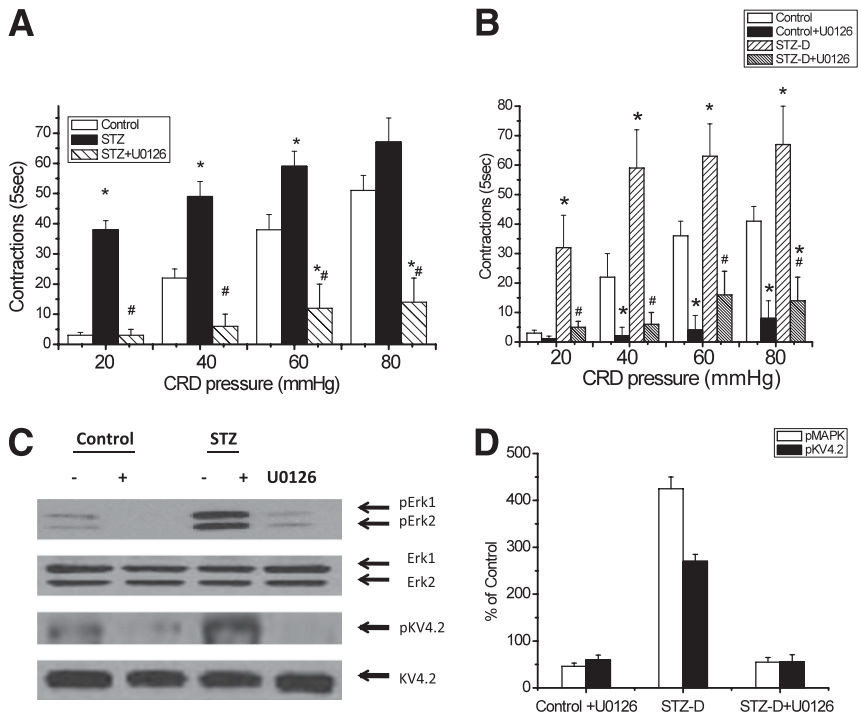

FIG. 7. In vivo demonstration that the MAPK cascade is involved in the modulation of visceromotor responses to CRD in control and STZ-D rats. *A* and *B*: Summary histogram shows that visceromotor responses to CRD (20–60 mmHg) were significantly elevated in STZ-D rats. Enhanced visceromotor responses to CRD were normalized by intravenous (*A*) and intrathecal (5 μg in 0.5 μL; *B*) administration of U0126 in the STZ-D rats (n = 6 and n = 4, respectively). Data are presented as means ± SE. *$P < 0.05$ compared with control rats; #$P < 0.05$ compared with the STZ-D before U0126 treatment. *C*: Western blots show that intravenous administration of U0126 reduced the levels of p-MAPK and p-K_V4.2 but not total MAPK or K_V4.2 in both control and STZ-D rats. The immunoblot is representative of four experiments. *D*: Summary histogram shows the effect of intravenous U0126 on the levels of p-MAPK and p-K_V4.2 (n = 4) in control and STZ-D rats. *$P < 0.05$ compared with DRG neurons from control rats.

concept and design, analysis and interpretation of data, drafting of the manuscript, critical revision of the manuscript for important intellectual content, and obtaining funding.

REFERENCES

1. Beyak MJ, Bulmer DC, Sellers D, Grundy D. Impairment of rectal afferent mechanosensitivity in experimental diabetes in the rat. Neurogastroenterol Motil 2009;21:678–681
2. Caruana BJ, Wald A, Hinds JP, Eidelman BH. Anorectal sensory and motor function in neurogenic fecal incontinence. Comparison between multiple sclerosis and diabetes mellitus. Gastroenterology 1991;100:465–470
3. Vinik AI, Maser RE, Mitchell BD, Freeman R. Diabetic autonomic neuropathy. Diabetes Care 2003;26:1553–1579
4. Wald A, Tunuguntla AK. Anorectal sensorimotor dysfunction in fecal incontinence and diabetes mellitus. Modification with biofeedback therapy. N Engl J Med 1984;310:1282–1287
5. McHugh JM, McHugh WB. Diabetes and peripheral sensory neurons: what we don't know and how it can hurt us. AACN Clin Issues 2004;15:136–149
6. Gold MS, Shuster MJ, Levine JD. Characterization of six voltage-gated K^+ currents in adult rat sensory neurons. J Neurophysiol 1996;75:2629–2646
7. Scroggs RS, Todorovic SM, Anderson EG, Fox AP. Variation in IH, IIR, and ILEAK between acutely isolated adult rat dorsal root ganglion neurons of different size. J Neurophysiol 1994;71:271–279
8. Connor JA, Stevens CF. Voltage clamp studies of a transient outward membrane current in gastropod neural somata. J Physiol 1971;213:21–30
9. Chien LY, Cheng JK, Chu D, Cheng CF, Tsaur ML. Reduced expression of A-type potassium channels in primary sensory neurons induces mechanical hypersensitivity. J Neurosci 2007;27:9855–9865
10. Phuket TRN, Covarrubias M. Kv4 channels underlie the subthreshold-operating A-type K^+-current in nociceptive dorsal root ganglion neurons. Front Mol Neurosci 2009;2:2–14
11. Biessels G, Gispen WH. The calcium hypothesis of brain aging and neurodegenerative disorders: significance in diabetic neuropathy. Life Sci 1996;59:379–387
12. Biessels GJ, ter Laak MP, Hamers FP, Gispen WH. Neuronal Ca^{2+} disregulation in diabetes mellitus. Eur J Pharmacol 2002;447:201–209
13. Hall KE, Sima AA, Wiley JW. Voltage-dependent calcium currents are enhanced in dorsal root ganglion neurones from the Bio Bred/Worchester diabetic rat. J Physiol 1995;486:313–322
14. Hall KE, Liu J, Sima AA, Wiley JW. Impaired inhibitory G-protein function contributes to increased calcium currents in rats with diabetic neuropathy. J Neurophysiol 2001;86:760–770
15. Kruglikov I, Gryshchenko O, Shutov L, Kostyuk E, Kostyuk P, Voitenko N. Diabetes-induced abnormalities in ER calcium mobilization in primary and secondary nociceptive neurons. Pflugers Arch 2004;448:395–401
16. Orrenius S, Zhivotovsky B, Nicotera P. Regulation of cell death: the calcium-apoptosis link. Nat Rev Mol Cell Biol 2003;4:552–565
17. Christianson JA, Traub RJ, Davis BM. Differences in spinal distribution and neurochemical phenotype of colonic afferents in mouse and rat. J Comp Neurol 2006;494:246–259
18. Grabauskas G, Song I, Zhou SY, Owyang C. Electrophysiological identification of glucose-sensing neurons in rat nodose ganglia. J Physiol 2010; 588:617–632
19. Chen SL, Wu XY, Cao ZJ, et al. Subdiaphragmatic vagal afferent nerves modulate visceral pain. Am J Physiol Gastrointest Liver Physiol 2008;294: G1441–G1449
20. Levy J, Gavin JR 3rd, Sowers JR. Diabetes mellitus: a disease of abnormal cellular calcium metabolism? Am J Med 1994;96:260–273
21. Hoffman DA, Johnston D. Downregulation of transient K^+ channels in dendrites of hippocampal CA1 pyramidal neurons by activation of PKA and PKC. J Neurosci 1998;18:3521–3528
22. Averill S, Delcroix JD, Michael GJ, Tomlinson DR, Fernyhough P, Priestley JV. Nerve growth factor modulates the activation status and fast axonal transport of ERK 1/2 in adult nociceptive neurones. Mol Cell Neurosci 2001;18:183–196
23. Yuan LL, Adams JP, Swank MJ, Sweatt JD, Johnston D. Protein kinase modulation of dendritic K^+ channels in hippocampus involves a mitogen-activated protein kinase pathway. J Neurosci 2002;22:4860–4868
24. Einat H, Yuan P, Gould TD, et al. The role of the extracellular signal-regulated kinase signaling pathway in mood modulation. J Neurosci 2003; 23:7311–7316

25. Robinson DR, McNaughton PA, Evans ML, Hicks GA. Characterization of the primary spinal afferent innervation of the mouse colon using retrograde labelling. Neurogastroenterol Motil 2004;16:113–124
26. Hunt SP, Mantyh PW. The molecular dynamics of pain control. Nat Rev Neurosci 2001;2:83–91
27. Schneider U, Quasthoff S, Mitrović N, Grafe P. Hyperglycaemic hypoxia alters after-potential and fast K^+ conductance of rat axons by cytoplasmic acidification. J Physiol 1993;465:679–697
28. Fernyhough P, Gallagher A, Averill SA, et al. Aberrant neurofilament phosphorylation in sensory neurons of rats with diabetic neuropathy. Diabetes 1999;48:881–889
29. Purves T, Middlemas A, Agthong S, et al. A role for mitogen-activated protein kinases in the etiology of diabetic neuropathy. FASEB J 2001;15:2508–2514
30. Zhang Y, Dong C. Regulatory mechanisms of mitogen-activated kinase signaling. Cell Mol Life Sci 2007;64:2771–2789
31. Dai Y, Iwata K, Fukuoka T, et al. Phosphorylation of extracellular signal-regulated kinase in primary afferent neurons by noxious stimuli and its involvement in peripheral sensitization. J Neurosci 2002;22:7737–7745
32. Ji RR, Woolf CJ. Neuronal plasticity and signal transduction in nociceptive neurons: implications for the initiation and maintenance of pathological pain. Neurobiol Dis 2001;8:1–10
33. Daulhac L, Mallet C, Courteix C, et al. Diabetes-induced mechanical hyperalgesia involves spinal mitogen-activated protein kinase activation in neurons and microglia via *N*-methyl-D-aspartate-dependent mechanisms. Mol Pharmacol 2006;70:1246–1254
34. Cao XH, Byun HS, Chen SR, Cai YQ, Pan HL. Reduction in voltage-gated K^+ channel activity in primary sensory neurons in painful diabetic neuropathy: role of brain-derived neurotrophic factor. J Neurochem 2010;114:1460–1475